Acta Crystallographica Section A
Foundations of Crystallography
ISSN 0108-7673

Received 27 March 2000
Accepted 3 June 2000

Diffraction by one-dimensional paracrystals and perturbed lattices

R. P. Millane* and J. L. Eads

Whistler Center for Carbohydrate Research, and Computational Science and Engineering Program, Purdue University, West Lafayette, IN 47907-1160, USA. Correspondence e-mail: rmillane@purdue.edu

A detailed comparison of the one-dimensional paracrystalline and perturbed lattice models of disordered crystals, and their diffraction, is made. If noncumulative (thermal) disorder is added to the paracrystalline model, then the two models and their diffraction patterns are similar but not identical because of their different intersite statistics. However, they are identical in the limiting cases of either strong or weak correlations. Calculation of diffraction patterns shows that, with an appropriate choice of parameters, the two models give essentially identical diffraction for small crystallites and very similar diffraction for larger crystallites. An empirical relationship is derived between parameters of the two models such that they give similar diffraction patterns.

1. Introduction

Analysis of X-ray diffraction patterns from disordered crystalline materials is an important means of analyzing disorder in such systems (Welberry, 1985; Stroud & Millane, 1995*b*). Performing such an analysis requires both a statistical model of the disordered system and a method for calculating diffraction patterns based on the model. With these two components, one is able, at least in principle, to process diffraction data from a particular specimen to quantitatively characterize the kind and degree of disorder by estimating parameters of the statistical model.

Disordered crystalline systems can be conveniently described in terms of *lattice disorder* and *substitution disorder*. Substitution disorder consists of variations in the units located at each site of the crystal lattice. The variations could be due to the presence of different atoms or molecules at different sites, or to a single type of molecule adopting different orientations. Lattice disorder consists of variations in the positions of the lattice sites away from those of an ordered periodic lattice. Clearly, substitution disorder almost always introduces some degree of lattice disorder, although lattice disorder can be present in the absence of substitution disorder. We consider here only lattice disorder. The diffraction pattern from such a system is then equal to the Fourier transform of the molecule, modulated by the Fourier transform (or diffraction pattern) of the distorted lattice (the interference function). The distorted crystalline system and its diffraction properties are therefore characterized by the distorted lattice. In this paper, we compare the two primary models of distorted lattices, the paracrystal and the perturbed lattice, and their diffraction patterns.

The simplest model of lattice disorder involves independent distortions of the lattice sites away from those of a regular periodic lattice and is referred to variously as thermal disorder, disorder of the *first kind* (Hosemann & Bagchi, 1962) or uncorrelated disorder (Stroud & Millane, 1996). Although this model of disorder is useful in many situations (Millane & Stroud, 1991; Stroud & Millane, 1995*b*), it does not incorporate the dependence between distortions at neighboring lattice sites that are often characteristic, at least to some degree, of close-packed systems. To include dependence between the distortions at neighboring sites, the distortions must be correlated. The diffraction pattern from a material with uncorrelated disorder is equal to the sum of two components; one consisting of sharp Bragg reflections characteristic of the underlying average undistorted lattice and a continuous component resulting from the disorder (Stroud & Millane, 1995*a*). In the case of correlated disorder however, the diffraction cannot be written as the sum of two such components and is characterized by peaks that broaden with increasing scattering angle and merge into the continuous diffraction (Stroud & Millane, 1996).

Although real systems are generally three dimensional, construction of general models of disorder in more than one dimension is plagued by a number of fundamental difficulties (Welberry *et al.*, 1980; Welberry, 1985; Stroud & Millane, 1996). Disordered materials are therefore often studied by analyzing the diffraction along particular directions in reciprocal space and the diffraction interpreted in terms of a one-dimensional model to characterize the disorder in the corresponding directions in real space. This is an approximate approach but is sometimes sufficiently accurate in practice. One-dimensional models of disorder, and their resulting diffraction patterns, are therefore of utility in many applications. Furthermore, systems such as polymer and layered structures in which the disorder is fundamentally one dimensional can be accurately analyzed using a one-dimensional model (Hendricks & Teller, 1942;

Barakat, 1987; Inouye, 1994). For example, Egelman & DeRosier (1982) and Mu *et al.* (1997) have used a one-dimensional model to study cumulative angular disorder in actin and sickle-cell hemoglobin fibers, respectively. Biswas & Blackwell (1988) have used a one-dimensional model to calculate fiber diffraction patterns from random copolymers. One-dimensional models are also used to analyze X-ray peak shapes to determine disorder and crystallite size of crystalline polymers (Hall & Somashekar, 1991; Somashekar & Somashekarappa, 1997). One-dimensional models of disorder are therefore of fundamental and practical interest and are the subject of this paper.

Two principal models have been used to describe disordered crystalline materials: the paracrystal and the perturbed lattice. The paracrystal model was developed by Hosemann and co-workers (Hosemann & Bagchi, 1962) and has been widely used to analyze diffraction from disordered materials such as polymers, glasses and alloys (Hosemann & Hindeleh, 1995). Development of the paracrystal proceeds from the intuitive viewpoint that molecules (or atoms) in a growing crystal are positioned relative to their predecessors. Starting at a fixed point, sites are added to the lattice in succession by displacing each relative to its predecessor by a random distance. If the distances are normally distributed, then the average intensity diffracted by the random lattice is easily calculated. The perturbed lattice, rather than describing a distorted lattice in terms of the statistics of the relative positions of its sites, describes the lattice in terms of the displacements of its sites away from those of a periodic reference lattice (Welberry *et al.*, 1980; Welberry, 1985; Stroud & Millane, 1996). This produces a rather general model of disorder if one allows the displacements at neighboring lattice sites to be correlated with each other.

Both the paracrystal and the perturbed lattice models are well defined in one dimension but are well defined only under restricted conditions in more than one dimension (Welberry, 1985). In particular, in a two- or three-dimensional lattice there are many more cell edges (with which the random variables of the paracrystal are associated) than lattice points, implying that conditional dependencies must be imposed on the distributions (Hammersley, 1967). The perturbed lattice model avoids this difficultly by working with the positions of the lattice points rather than with the vectors between them. In multiple dimensions, the perturbed lattice model is more flexible and can be used to represent a wider variety of distorted lattices than the paracrystal while maintaining stationary statistics, although a completely general model is still difficult to construct (Welberry, 1985).

Since both models are well defined in one dimension and since the paracrystal has a long history of applications, it is of interest to compare the two models and their diffraction patterns. Welberry *et al.* (1980) have compared the one-dimensional (as well as the two-dimensional) paracrystal and perturbed lattice models. They demonstrate that as the distortions at adjacent sites in a one-dimensional perturbed lattice become highly correlated, and the single-site variances increase in an appropriate way, the perturbed lattice model approaches the paracrystalline model. A more detailed and complete comparison of the two models is presented here. We show that, if the one-dimensional paracrystal is generalized by adding a thermal disorder component, it has similar characteristics to the perturbed lattice, and the statistics of the two models and their diffraction patterns are studied in detail. The finite one-dimensional paracrystalline and perturbed lattice models and their diffraction patterns are described in the next two sections. The statistics and diffraction patterns from the two models are compared in the following section, and the results discussed in the final section.

2. The paracrystal

The paracrystalline model of disorder was first described by Hosemann and co-workers (Hosemann, 1950; Hosemann & Bagchi, 1962) and has since been quite widely used as a model of disorder, particularly for polymers and metals. The general paracrystalline model in more than one dimension suffers from a number of difficulties with consistency of the statistics and has therefore been the subject of some controversy (Brämer, 1975). However, the model is well defined in one dimension, which is the case with which we are concerned here. In the paracrystal model, a distorted lattice is described in terms of random displacements of a lattice site from its neighboring site. The model incorporates the intuitively satisfying concept of a disordered lattice being built sequentially, one lattice point at a time. The distortions of the lattice are therefore 'cumulative', and the disorder is sometimes referred to as disorder of the *second kind* (Hosemann & Bagchi, 1962). The diffraction from a paracrystal has Bragg reflections that increase in width with increasing scattering angle, a phenomenon that is often observed but is not accounted for by models of uncorrelated disorder.

The one-dimensional paracrystal usually incorporates only independent variations in the distances between adjacent sites. For reasons that will become apparent later, we consider a more general model that also includes independent distortions in the coordinates of the sites. The model can then be thought of as a pure paracrystal with superimposed thermal disorder. We refer to this as the *generalized paracrystal*. Let x_j be the coordinate of the jth site of a distorted lattice with N sites labeled $j = 0, 1, \ldots, N-1$ and average lattice spacing a. The coordinates of a generalized paracrystal are given by

$$x_j = ja + d_j^{\rm nc} + \sum_{k=0}^{j} d_k^{\rm pc}, \qquad (1)$$

where the $d_k^{\rm pc}$ are the random 'paracrystalline', or cumulative, displacements, the $d_j^{\rm nc}$ are the 'noncumulative' (thermal) displacements and we take $d_0^{\rm pc} = 0$. The $d_k^{\rm pc}$ and $d_j^{\rm nc}$ are independent, and each are uncorrelated zero-mean normally distributed random variables, with variances $\sigma_{\rm pc}^2$ and $\sigma_{\rm nc}^2$, respectively.

The diffraction by a lattice is given by

$$F(u) = \sum_{j=0}^{N-1} \exp(i2\pi u x_j), \qquad (2)$$

where u is the continuous coordinate in reciprocal space. The observed diffracted intensity $I(u)$ is given by the diffracted intensity averaged over all realizations of the lattice, or over all x_j, *i.e.*

$$I(u) = \langle |F(u)|^2 \rangle = \sum_{j=0}^{N-1} \sum_{k=0}^{N-1} \langle \exp[i2\pi u(x_j - x_k)] \rangle. \quad (3)$$

Using (1) and (3) gives the intensity diffracted by the paracrystal as

$$I_{\rm pc}(u) = \sum_{j=0}^{N-1} \sum_{k=0}^{N-1} \exp[i2\pi ua(j-k)] \times \left\langle \exp\left[i2\pi u \left(\sum_{l=0}^{j} d_l^{\rm pc} - \sum_{l=0}^{k} d_l^{\rm pc} \right) \right] \right\rangle \times \langle \exp[i2\pi u(d_j^{\rm nc} - d_k^{\rm nc})] \rangle. \quad (4)$$

The quantity $(d_j^{\rm nc} - d_k^{\rm nc})$ is normally distributed with zero mean and variance $2\sigma_{\rm nc}^2$, so that (Papoulis, 1991)

$$\langle \exp[i2\pi u(d_j^{\rm nc} - d_k^{\rm nc})] \rangle = \exp(-4\pi^2 u^2 \sigma_{\rm nc}^2). \quad (5)$$

The first average in (4) needs to be handled more carefully since some of the $d_l^{\rm pc}$ are not independent. Evaluating the average (Appendix A) and using (4), (5) and (33) gives the intensity diffracted by the finite generalized paracrystal as

$$I_{\rm pc}(u) = N + 2 \sum_{j=1}^{N-1} (N-j) \exp[-2\pi^2 u^2 (2\sigma_{\rm nc}^2 + \sigma_{\rm pc}^2 j)] \times \cos(2\pi uaj). \quad (6)$$

The summation in (6) can be evaluated in closed form for $N \to \infty$ (Hosemann & Bagchi, 1962) or for finite N (Mu, 1998). For our purposes however, it is useful to retain the form (6) because of its similarity to the expression for diffraction by the perturbed lattice derived in the next section.

If there is no paracrystalline disorder ($\sigma_{\rm pc} = 0$), then (6) can be written in the form

$$I_{\rm pc}(u) = N[1 - \exp(-4\pi^2 u^2 \sigma_{\rm nc}^2)] + \exp(-4\pi^2 u^2 \sigma_{\rm nc}^2) \times \sum_{j=0}^{N-1} \varepsilon_j (N-j) \cos(2\pi uaj), \quad (7)$$

where $\varepsilon_j = 1$ for $j = 0$ and $\varepsilon_j = 2$ for $j > 0$, *i.e.* the intensity is the sum of a continuous component that increases with increasing u and a Bragg component (the interference function of the finite unperturbed lattice) that decreases with increasing u. These are the characteristics of uncorrelated, or thermal, disorder.

Diffraction patterns from a one-dimensional generalized paracrystal for $N = 10$ are calculated using (6) and shown in Fig. 1. All diffraction patterns are scaled to the first peak. We take $a = 1$ for all the examples so that the variances are normalized values. Diffraction by the usual paracrystal (no noncumulative disorder) is shown in Fig. 1(a) for different degrees of disorder (different $\sigma_{\rm pc}$). For small disorder, the diffraction pattern is dominated by Bragg peaks that broaden gradually with increasing scattering angle (top), and as the disorder ($\sigma_{\rm pc}$) increases the peaks broaden more rapidly with increasing scattering angle and merge with a continuous background that increases to an asymptotic value at high scattering angle. As the disorder increases, the angle out to which sharp peaks occur decreases. At no point does the diffraction pattern completely separate into a sum of Bragg and continuous components. Diffraction from a generalized paracrystal with noncumulative disorder is shown in Fig. 1(b). The paracrystalline disorder is fixed at $\sigma_{\rm pc} = 0.05$, and the noncumulative disorder increases from $\sigma_{\rm nc} = 0$ to 0.1 from the top of the figure to the bottom. As the noncumulative disorder increases, the peaks narrow at their bases

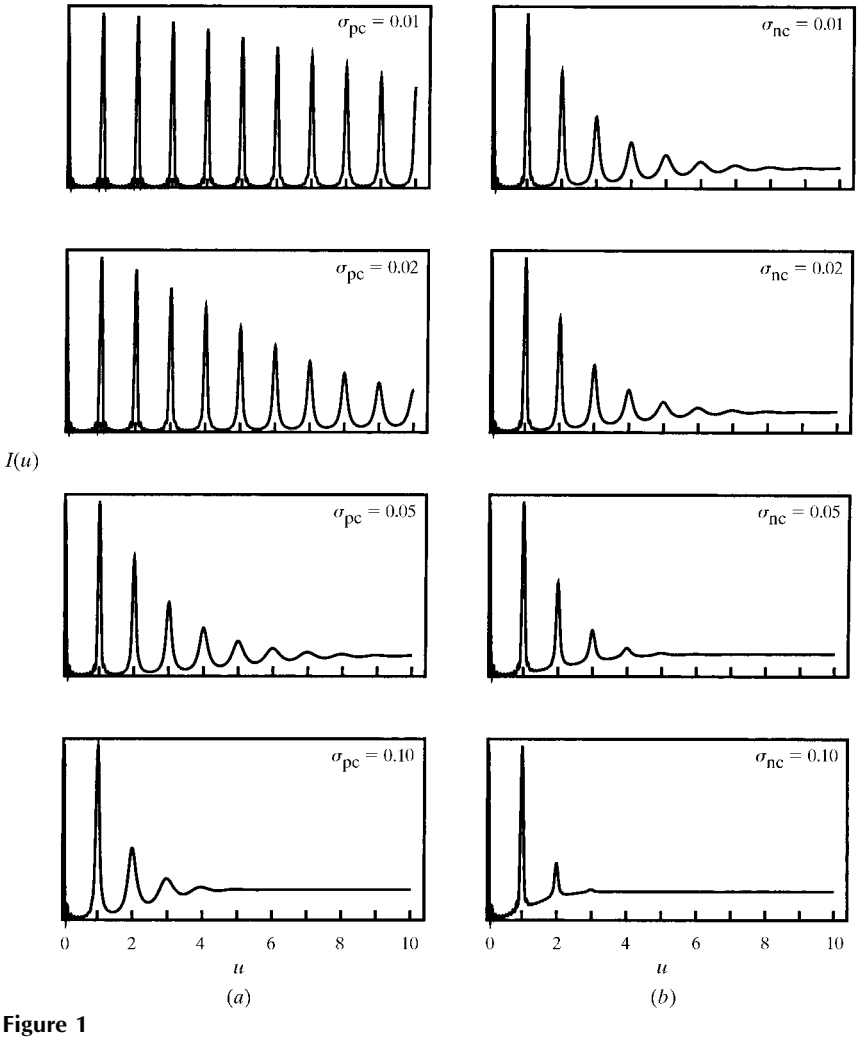

Figure 1
Diffraction patterns from generalized paracrystalline lattices for $N = 10$ for (a) no noncumulative disorder ($\sigma_{\rm nc} = 0$) and (b) with noncumulative disorder (with $\sigma_{\rm pc} = 0.05$), for the values of $\sigma_{\rm pc}$ and $\sigma_{\rm nc}$ shown.

and, when the noncumulative disorder dominates the paracrystalline disorder, the diffraction pattern approaches one of uncorrelated disorder, *i.e.* a sharp Bragg component on a continuous background (bottom of the figure). Since the paracrystalline disorder is constant and the noncumulative disorder increases, the total disorder increases and the scattering angle out to which peaks appear decreases from the top of the figure to the bottom.

3. The perturbed lattice

The perturbed lattice model of a disordered crystal has been studied by Welberry & Galbraith (1973) and Welberry *et al.* (1980). In this model, a distorted lattice is described in terms of the correlated displacements of its sites away from those of a periodic reference lattice rather than in terms of displacements between adjacent sites as in the case of the paracrystal (Welberry *et al.*, 1980; Welberry, 1985; Stroud & Millane, 1996). This produces a rather general model of disorder. It is generally assumed that the statistics of the lattice are stationary and that only random variables at neighboring sites interact. A one-dimensional perturbed lattice with only nearest-neighbor interactions can be described as a simple Markov chain (Welberry *et al.*, 1980).

The coordinate of the jth site of a perturbed lattice is given by

$$x_j = ja + d_j, \tag{8}$$

where the d_j are zero-mean random displacements and we take $x_0 = d_0 = 0$. We take the d_j to be jointly normal with only nearest-neighbor interactions so the statistics of the lattice are described by the joint density

$$P(d_j, d_{j-1}) = \frac{1}{2\pi\sigma_{\rm pl}^2(1-\rho^2)^{1/2}} \exp\left[-\frac{d_j^2 - 2\rho d_j d_{j-1} + d_{j-1}^2}{2\sigma_{\rm pl}^2(1-\rho^2)}\right], \tag{9}$$

where the variance and correlation coefficient are

$$\sigma_{\rm pl}^2 = \langle d_j^2 \rangle \quad \text{and} \quad \rho = \langle d_j d_{j-1} \rangle / \sigma_{\rm pl}^2, \tag{10}$$

$\langle \ldots \rangle$ denotes the ensemble average and the subscript pl denotes the 'perturbed lattice'. Since the perturbed lattice is a Gaussian Markov chain, the correlation ρ_k between d_j and d_{j+k} is [Welberry *et al.* (1980); Appendix *B*]

$$\rho_k = \rho^{|k|}, \tag{11}$$

and the joint density of d_j and d_{j+k} is identical to (9) with ρ replaced by $\rho^{|k|}$.

Using (3) and (8) gives the intensity diffracted by the perturbed lattice as

$$I_{\rm pl}(u) = \sum_{j=0}^{N-1} \sum_{k=0}^{N-1} \exp[i2\pi ua(j-k)] \langle \exp[i2\pi u(d_j - d_k)] \rangle. \tag{12}$$

The quantity $(d_j - d_k)$ is normally distributed with zero mean and variance

$$\langle (d_j - d_k)^2 \rangle = 2\sigma_{\rm pl}^2 - 2\sigma_{\rm pl}^2 \rho_{|j-k|} = 2\sigma_{\rm pl}^2 (1 - \rho^{|j-k|}),$$

so that

$$I_{\rm pl}(u) = \sum_{j=0}^{N-1} \sum_{k=0}^{N-1} \exp[i2\pi ua(j-k)] \exp[-4\pi^2 u^2 \sigma_{\rm pl}^2 (1 - \rho^{|j-k|})]. \tag{13}$$

The terms with equal $(j-k)$ in (13) can be combined so that

$$I_{\rm pl}(u) = N + 2\sum_{j=1}^{N-1} (N-j) \exp[-4\pi^2 u^2 \sigma_{\rm pl}^2 (1 - \rho^j)] \cos(2\pi uaj). \tag{14}$$

If the distortions are uncorrelated ($\rho = 0$), the diffracted intensity can be written in the same form as (7) with $\sigma_{\rm nc}$ replaced by $\sigma_{\rm pl}$. The two models are therefore identical for $\sigma_{\rm pc} = 0$ and $\rho = 0$.

Diffraction patterns for one-dimensional perturbed lattices for $N = 10$ are calculated using (14) and shown in Fig. 2. Diffraction from lattices with only uncorrelated disorder ($\rho = 0$) are shown in Fig. 2(*a*) for small disorder at the top and $\sigma_{\rm pl}$ increasing down the figure. Since the disorder is uncorrelated, the diffraction separates into a sharp Bragg component on a continuous background and the widths of the Bragg reflections are independent of scattering angle. The amplitudes of the Bragg reflections decrease more rapidly with scattering angle as the disorder increases and there is an associated increase in the amplitude of the continuous component. Diffraction patterns from a perturbed lattice with correlated disorder and fixed $\sigma_{\rm pl}$ are shown in Fig. 2(*b*), the degree of correlation increasing from $\rho = 0$ at the top to $\rho = 0.9$ at the bottom of the figure. As the correlation increases, the Bragg peaks broaden with increasing scattering angle and merge into the continuous background at high angle. As the correlation coefficient increases, the lattice becomes less disordered and the diffraction peaks persist out to higher scattering angle.

4. Comparison of the paracrystal and the perturbed lattice

4.1. Statistics

The generalized paracrystal and the perturbed lattice are different statistical models of a disordered lattice. However, both models are stationary Gaussian processes and can therefore be described by the variances of the kth-nearest-neighbor intersite distances $(x_{j+k} - x_j)$ for all k. Referring to (1), (8) and (11) shows that these variances, $\sigma_k^2 = \langle (x_{j+k} - x_j - ka)^2 \rangle$, are given by

$$\sigma_k^{\rm pc\,2} = |k|\sigma_{\rm pc}^2 + 2\sigma_{\rm nc}^2 \tag{15}$$

for the generalized paracrystal and

$$\sigma_k^{\rm pl\,2} = 2\sigma_{\rm pl}^2 (1 - \rho^{|k|}) \tag{16}$$

for the perturbed lattice. Note that the largest value of k is $N-1$. Equations (15) and (16) highlight the difference between the two models. The variance increases linearly with the number of intervening sites for the generalized paracrystal, whereas for the perturbed lattice it asymptotically

approaches $2\sigma_{\rm pl}^2$. These relationships are shown in Fig. 3. Two limiting cases correspond to

$$\begin{aligned}\sigma_{\rm pc} = 0 &\Rightarrow \sigma_k^{\rm pc\,2} = 2\sigma_{\rm nc}^2 \\ \rho = 0 &\Rightarrow \sigma_k^{\rm pl\,2} = 2\sigma_{\rm pl}^2\end{aligned} \tag{17}$$

for uncorrelated disorder (Fig. 3*b*) and

$$\begin{aligned}\sigma_{\rm nc} = 0 &\Rightarrow \sigma_k^{\rm pc\,2} = |k|\sigma_{\rm pc}^2 \\ \rho \to 1 &\Rightarrow \sigma_k^{\rm pl\,2} \to 2|k|\sigma_{\rm pl}^2(1-\rho) \qquad \text{for small } k\end{aligned} \tag{18}$$

for highly correlated disorder (Fig. 3*c*). For uncorrelated disorder, the two models are identical as shown in Fig. 3(*b*). For highly correlated disorder, the perturbed lattice becomes more ordered as ρ approaches unity unless $\sigma_{\rm pl}$ is increased. This is illustrated in Fig. 3(*c*) for which $\rho = 0.995$, $\sigma_{\rm pl} = 10\sigma_{\rm pc}$ and $\sigma_{\rm nc} = 0$. In the limit $\rho \to 1$, $\sigma_k^{\rm pl\,2}$ depends linearly on k, the same as for the paracrystal with no noncumulative (thermal) disorder (Fig. 3*c*), for small k. Note that k is bounded by $N-1$, so that the similarity of the two models is expected to decrease for larger N, for which larger values of k occur.

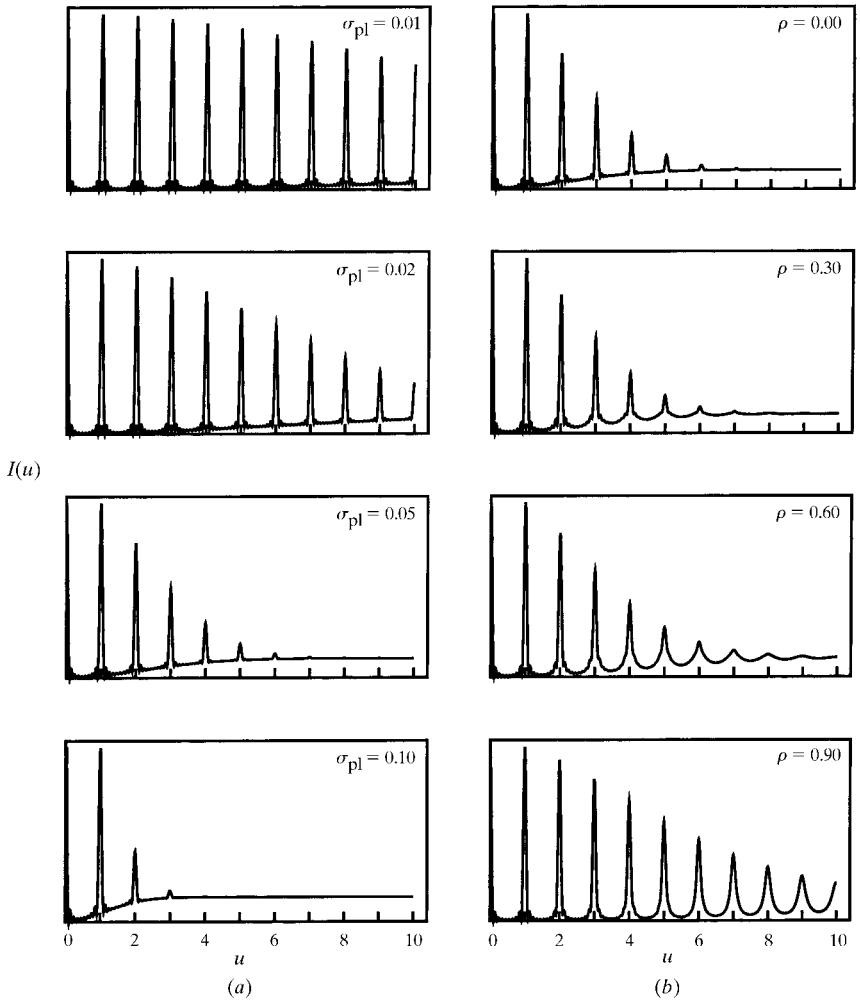

Figure 2
Diffraction patterns from perturbed lattices for $N = 10$ for (*a*) uncorrelated ($\rho = 0$) and (*b*) correlated (with $\sigma_{\rm pl} = 0.05$) disorder, for the values of $\sigma_{\rm pl}$ and ρ shown.

The different forms of the k dependence of σ_k^2 for the two models means that parameters cannot be chosen to make the two models identical, *i.e.* it is not possible to obtain $\sigma_k^{\rm pc} = \sigma_k^{\rm pl}$ for all k. However, both models incorporate similar characteristics and so are expected to exhibit qualitatively similar behavior (as evidenced by the diffraction patterns shown in Figs. 1 and 2) for appropriate choices of the parameters. It is convenient to denote the standard deviations of the nearest-neighbor intersite distances by $\delta_{\rm pc}^2 = \sigma_1^{\rm pc\,2}$ and $\delta_{\rm pl}^2 = \sigma_1^{\rm pl\,2}$, so that

$$\delta_{\rm pc}^2 = \sigma_{\rm pc}^2 + 2\sigma_{\rm nc}^2 \tag{19}$$

and

$$\delta_{\rm pl}^2 = 2\sigma_{\rm pl}^2(1-\rho), \tag{20}$$

and to define R by

$$R = \sigma_{\rm nc}^2/\sigma_{\rm pc}^2, \tag{21}$$

i.e. the noncumulative variance relative to the paracrystalline variance for the generalized paracrystal.

We now investigate relationships between the parameters of the two models that tend to make them similar. From Fig. 3, this will occur when the differences between $\sigma_k^{\rm pc\,2}$ and $\sigma_k^{\rm pl\,2}$, averaged over $1 \le k \le N-1$, are minimized. A direct minimization does not lead to a tractable result, but a simple indicative relationship is obtained using the following approximate approach. We first apply the constraint that the variances of the distances between nearest neighbors are the same for both models, *i.e.*

$$\delta_{\rm pc} = \delta_{\rm pl} = \delta. \tag{22}$$

Referring to Fig. 3(*d*), we write

$$\sigma_{N-1}^{\rm pc\,2} = \delta^2 + l = \delta^2 + \alpha(2\sigma_{\rm pl}^2 - \delta^2), \tag{23}$$

where l is shown in Fig. 3(*d*). The value of α that minimizes the difference between $\sigma_k^{\rm pc\,2}$ and $\sigma_k^{\rm pl\,2}$ summed over k will in general depend on N, but inspection of Fig. 3(*d*) shows that it satisfies $\alpha < 2$. Using (15) and (19)–(22) to rewrite (23) in terms of ρ and R gives

$$\rho = \frac{N-2}{N-2+\alpha+2\alpha R}. \tag{24}$$

For $N \gg 1$ and $R \gg 1$, since $\alpha < 2$, (24) can be approximated by

$$\rho \approx \frac{N}{N+2\alpha R}. \tag{25}$$

Since the form of α is unknown, (24) and (25) cannot be used directly to determine values of ρ and R that make the two models similar. However, the functional form suggested by (25) is useful for developing an

empirical relationship between ρ and R such that the two models give similar diffraction patterns, as is shown in §4.2.

4.2. Diffraction patterns

Equations (6) and (14) for diffraction by the generalized paracrystal and the perturbed lattice cannot be compared directly because of the different j dependence of the arguments of the exponential terms in the summations. The nature of the diffraction pattern from the generalized paracrystal depends on the parameters σ_{pc} and σ_{nc}, and that from the perturbed lattice on σ_{pl} and ρ (for fixed N in both cases). Reference to Figs. 1 and 2 shows that these parameters affect diffraction by the two models differently. However, the intensity diffracted from an array of points depends only on the relative positions of the points $(x_j - x_k)$ [equation (2)]. We have shown elsewhere (Stroud & Millane, 1996) that, for fixed $\delta^2 = \langle (x_j - x_{j-1} - a)^2 \rangle$ (as defined above), diffraction patterns from perturbed lattices are similar in the sense that peaks extend out to approximately the same scattering angle, irrespective of the values of other parameters of the disorder. It therefore makes sense to parameterize the problem in terms of δ. The significance of δ is illustrated in Fig. 4 which shows diffraction patterns from generalized paracrystals (left) and perturbed lattices (right) with $\delta = 0.05$ and values of σ_{nc} and ρ as shown. The overall diffraction is similar in all of these plots, detailed differences being in the shapes of the peaks. In the figure, σ_{nc} decreases from top to bottom for the generalized paracrystal and ρ increases from top to bottom for the perturbed lattice, so that for both models the degree of correlation between the distortions at adjacent sites increases down the figure. When plotted in this way, the similarities between the two models become quite apparent. We therefore set $\delta_{pc} = \delta_{pl} = \delta$ to obtain similar diffraction by the two models.

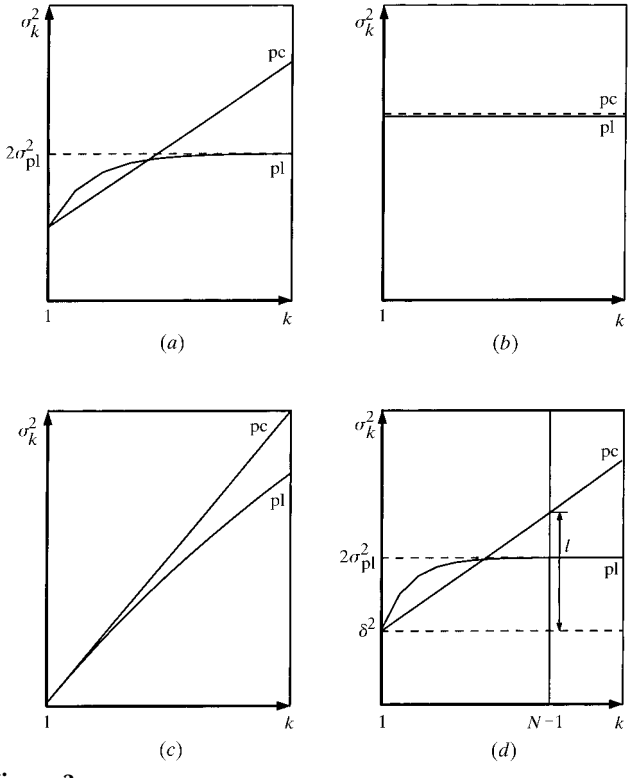

Figure 3
The dependence of σ_k^{pc2} and σ_k^{pl2} on k for (*a*) the general case, (*b*) uncorrelated disorder, (*c*) highly correlated disorder and (*d*) the construction for equation (24).

A second parameter (aside from δ) is required for each model, and it is convenient to use R for the generalized paracrystal (as defined above) and ρ for the perturbed lattice. Writing (6) and (14) in terms of these parameters gives

$$I_{pc}(u) = N + 2\sum_{j=1}^{N-1}(N-j)\exp\left[-2\pi^2u^2\delta^2\left(\frac{2R+j}{2R+1}\right)\right] \times \cos(2\pi uaj) \quad (26)$$

and

$$I_{pl}(u) = N + 2\sum_{j=1}^{N-1}(N-j)\exp\left[-2\pi^2u^2\delta^2\left(\frac{1-\rho^j}{1-\rho}\right)\right] \times \cos(2\pi uaj). \quad (27)$$

Inspection of (26) and (27) shows that differences are due to the different j dependences of the factors in the brackets in the exponential functions. The question is, can the diffraction by the two models be made similar by appropriate choices of ρ and R? To answer this question, diffraction patterns were calculated using (26) and (27), and values of ρ and R determined that make the diffracted intensities for the two models as close as possible.

To conduct such an analysis, it is necessary to consider the range of parameter values that are relevant in practice so that the results apply to a wide range of real systems. Measurements based on the paracrystalline model of disorder in some polymer systems, glasses and alloys show values of δ varying between about 0.01 and 0.15 (Baltá-Calleja & Hosemann, 1980). Experiments also show that the sizes of disordered crystallites usually satisfy the so-called 'α^* rule', $N = \alpha^{*2}/g^2$ (Baltá-Calleja & Hosemann, 1980), where g is the standard deviation (normalized to the average spacing) in the paracrystalline model (with only cumulative disorder) and $0.1 \lesssim \alpha^* \lesssim 0.2$. We associate g with δ and, for the values of δ described above, a representative range for N is $5 < N < 50$ and we consider N in this range. Since larger crystallites tend to have smaller distortions, the maximum value of δ that we consider decreases with increasing N (see the caption to Fig. 5). Since some systems exhibit mainly uncorrelated disorder and others highly correlated disorder, we consider a wide range of values of R to cover 'first-kind-dominated' and 'second-kind-dominated' disorder, and corresponding values of ρ.

For fixed values of δ and N in the ranges described above, R was fixed at different values and a search made for the value of ρ that minimizes the normalized r.m.s. difference Δ between the intensity diffracted by the two models, where

$$\Delta^2 = \int_0^{u_{\max}} [I_{\rm pl}(u) - I_{\rm pc}(u)]^2 \, {\rm d}u \Big/ \int_0^{u_{\max}} I_{\rm pl}^2(u) \, {\rm d}u \qquad (28)$$

and $u_{\max} = 1/2\delta$ is a value of u beyond which most structure in the diffraction pattern has died out. This gives relationships between ρ and R, for different values of δ and N, that make diffraction by the two models as similar as possible. The results of these calculations are shown in Fig. 5. The relationships between the ρ and R that minimize Δ are shown at the top of the figure (a) and the minimum difference $\Delta_{\rm min}$ between the diffraction patterns is shown as a function of R at the bottom of the figure (b). Note that R is plotted on a logarithmic scale. The curves are for the different values of N as shown and for the values of δ listed in the figure caption. Note first that Δ is small (<4%) for $N = 5$ and 10 but is larger for $N = 20$ and 50, particularly for R close to 1. Hence, for small values of N, the two models give almost identical diffraction patterns (for appropriate values of R and ρ). For larger values of N, the diffraction patterns are still fairly similar although the differences are more significant for $R \approx 1$. A second notable feature of Fig. 5 is that, for fixed N, the curves for the different values of δ are practically identical. The resulting relationships between ρ and R are therefore independent of δ.

In an attempt to find a single empirical relationship between ρ and R that describes the curves in Fig. 5(a), equation (25) with α constant (independent of N) was fitted to the curves by varying α. This gave a remarkably good fit. The fit was further improved by modifying (25) to the form

$$\rho = \frac{N^a}{N^a + bR}, \qquad (29)$$

and this function was found to fit the curves in Fig. 5(a) almost exactly with $a = 0.88$ and $b = 5.7$. The fit of this function is shown by the circles in Fig. 5(a). Equation (29) therefore gives an accurate empirical relationship between ρ and R such that the two models give similar diffraction patterns. Examples of diffraction patterns from the two models based on (29) are shown in Fig. 6, for $N = 10$ (a, b, c) and for the 'worst case' (largest $\Delta_{\rm min}$; $N = 50$, $R = 2$) in (d), for the values of R listed in the figure caption. The patterns in (a) and (c) are indistinguishable, in (b) the differences are quite small, and even in (d) they are quite small. This demonstrates that the diffraction patterns are almost identical when the statistics of the two models satisfy (29).

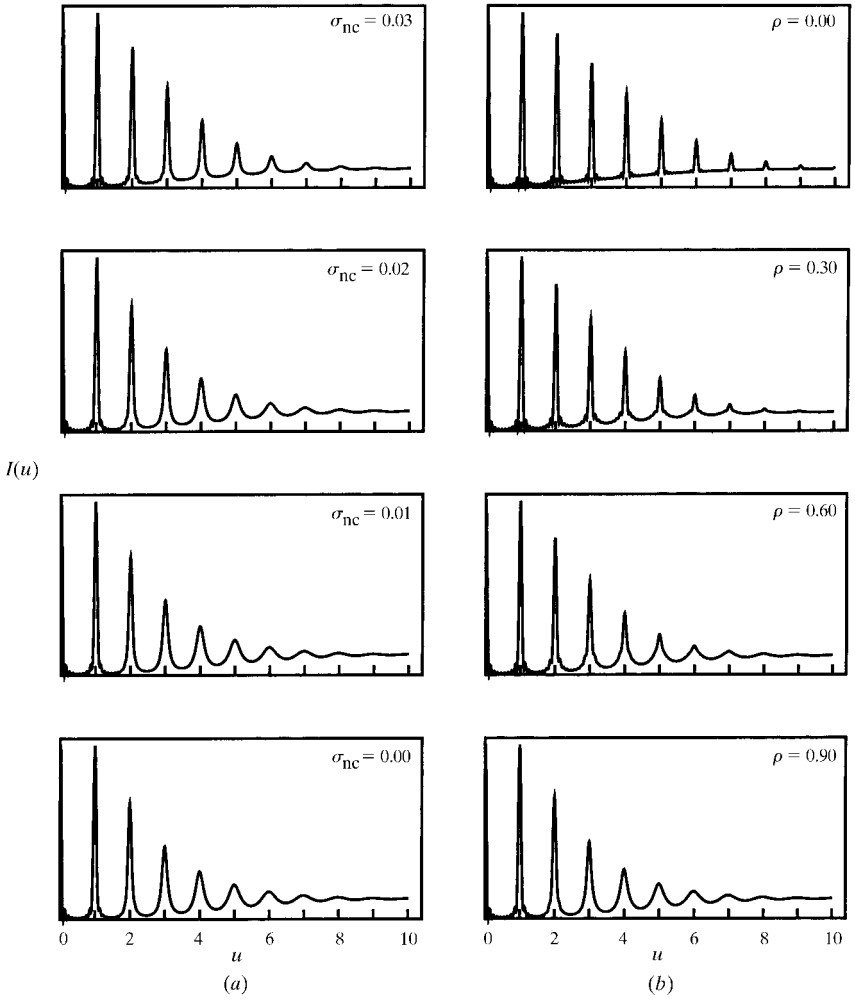

Figure 4
Diffraction patterns from (a) generalized paracrystalline lattices and (b) perturbed lattices for $N = 10$, $\delta = 0.05$ and values of $\sigma_{\rm nc}$ and ρ as shown.

We attempted to improve the fit between the two patterns for the 'worst case' as follows. Inspection of the patterns (shown again in Fig. 7a) shows that the single value of N results in ripples around the peaks that distort some of the peak shapes. In practice, however, mosaicity, a range of crystallite sizes and X-ray beam spread smear out these ripples. The effect of this is shown in Fig. 7(b) in which the diffraction patterns have been convolved with a Gaussian of standard deviation 0.01 to represent the smearing. The patterns in Fig. 7 have not been rescaled after smearing so that differences between the two models can be properly compared. Note also that the vertical scale has been expanded (clipping some of the first peaks) so that the small differences between the patterns are more evident. The smearing increases the similarity between the two patterns but the effect is small with $\Delta_{\rm min}$ being reduced only from 0.15 to 0.14. The assumption that $\delta_{\rm pc} = \delta_{\rm pl}$ gives similar diffraction patterns is clearly a good one for most of the cases considered since small values of $\Delta_{\rm min}$ are usually obtained. The effect of allowing $\delta_{\rm pc} \neq \delta_{\rm pl}$ was investigated for the 'worst case'. This was done by fixing $\delta_{\rm pc} = 0.05$ and varying ρ as well as $\delta_{\rm pl}$ to find the minimum value of Δ (after smearing the diffraction patterns as described above). This reduced $\Delta_{\rm min}$ to 0.09, with $\rho = 0.77$ and $\delta_{\rm pl} = 0.06$. The resulting diffraction patterns are shown

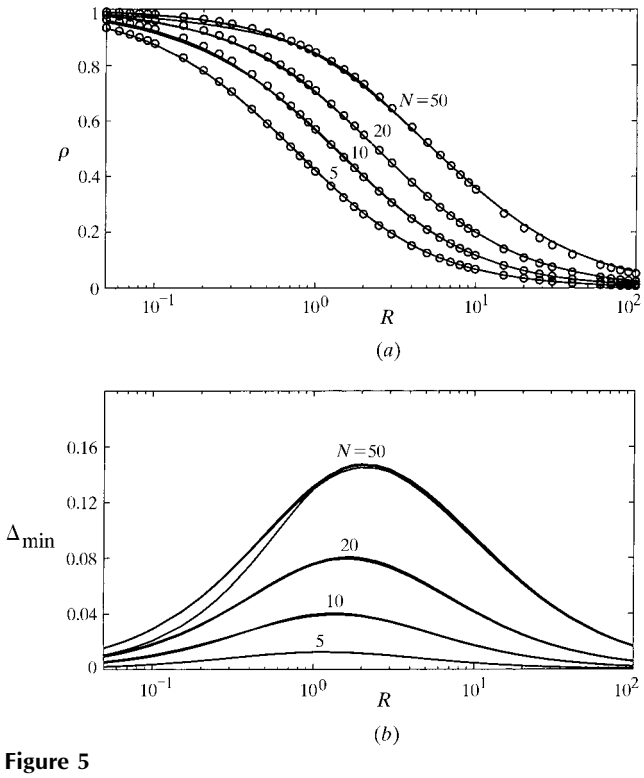

Figure 5
(*a*) The relationships between ρ and R that minimize Δ and (*b*) the minimum r.m.s. difference Δ_{min} between the intensity diffracted by the generalized paracrystal and perturbed lattices. The different sets of curves are for the different values of N as shown. The values of δ are for $N = 5$: $\delta = 0.02, 0.05, 0.10, 0.15$; for $N = 10$: $\delta = 0.02, 0.05, 0.10, 0.15$; for $N = 20$: $\delta = 0.01, 0.02, 0.05, 0.10$; and for $N = 50$: $\delta = 0.01, 0.02, 0.05, 0.10$. Circles show the function given by (29).

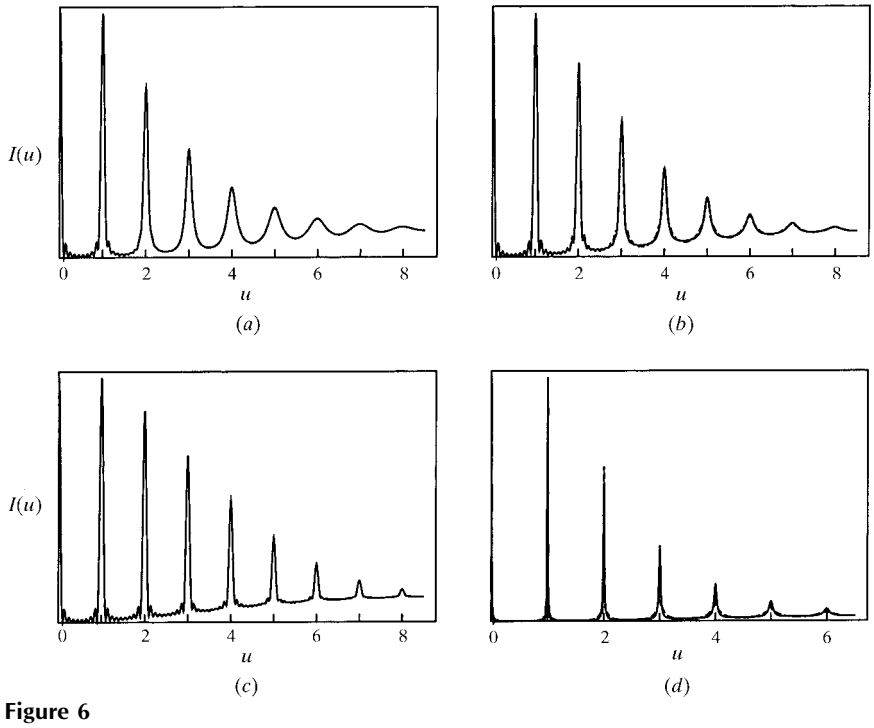

Figure 6
Diffraction patterns from generalized paracrystalline (full line) and perturbed (dashed line) lattices with $\delta_{pc} = \delta_{pl} = 0.05$ and ρ and R related by (29) for the values (*a*) $N = 10$, $R = 0.1$, $\rho = 0.93$, (*b*) $N = 10$, $R = 1$, $\rho = 0.57$, (*c*) $N = 10$, $R = 10$, $\rho = 0.12$ and (*d*) the 'worst case' $N = 50$, $R = 2$, $\rho = 0.72$.

in Fig. 7(*c*). Relaxing the constraint $\delta_{pc} = \delta_{pl}$ therefore does improve the match between the two diffraction patterns in the 'worst cases', although the improvement is not dramatic. Remaining differences between the two diffraction patterns are due to differences in the distributions of peak heights and widths with scattering angle (Fig. 7*c*) and are a result of the fundamental different statistical properties of the two models.

5. Discussion

The paracrystal and the perturbed lattice are two of the main models used to describe aspects of disordered crystalline materials. Each model has advantages and disadvantages. The paracrystal is conceptually easy to understand, is well defined in one dimension, has been widely used to analyze diffraction data from disordered materials but is not usefully generalizable to more than one dimension. The perturbed lattice, although maybe not quite as intuitive as the paracrystal initially, leads to a simpler model of a disordered lattice (due to its being defined relative to a fixed reference lattice) and its diffraction, is more easily generalized to more than one dimension, but has not yet seen as much application as the paracrystal.

A detailed comparison of the two models has been presented. If noncumulative (thermal) disorder is added to the paracrystalline model, then the two models share common features, both being able to represent a variety of disorder between uncorrelated and highly correlated distortions. The models are not identical because of different distributions of the variances of the intersite distances (Fig. 3). Despite this, an empirical relationship between the parameters of the two models has been determined that makes their diffraction patterns very similar for typical distortions and crystallite sizes. This leads to essentially identical diffraction patterns if the crystallites are small or for large crystallites if either cumulative or noncumulative disorder dominates. For larger crystallites and similar degrees of cumulative and noncumulative disorder ($R \approx 1$ or $\rho \approx 0.6$), the patterns are not identical but the differences between them are quite small.

The similarity of the diffraction patterns from the two models indicates that diffraction data are not able to tell one if a particular material under study is better described by one model than the other. Although the paracrystal has seen the most application in analyzing one-dimensional disordered systems, the results presented here indicate that use of the perturbed lattice would be just as, and probably more (since it includes the 'generalized' paracrystal), satisfactory.

Since the perturbed lattice is more easily generalized to more dimensions, these results lend support to use of the perturbed lattice model for describing disorder in multidimensional systems.

APPENDIX *A*
Evaluation of equation (4)

Depending on the values of j and k, some of the $d_l^{\rm pc}$ appearing in the first average in (4) may be identical and therefore not independent. The summation over k is separated into two parts so that the $d_l^{\rm pc}$ are independent in each, giving

$$I_{\rm pc}(u) = N + \exp(-4\pi^2u^2\sigma_{\rm nc}^2)\sum_{j=0}^{N-1}\left[\sum_{k=0}^{j-1}\exp[i2\pi ua(j-k)]\times\left\langle\exp\left(i2\pi u\sum_{l=k+1}^{j}d_l^{\rm pc}\right)\right\rangle + \sum_{k=j+1}^{N-1}\exp[i2\pi ua(j-k)]\left\langle\exp\left(-i2\pi u\sum_{l=j+1}^{k}d_l^{\rm pc}\right)\right\rangle\right]. \quad (30)$$

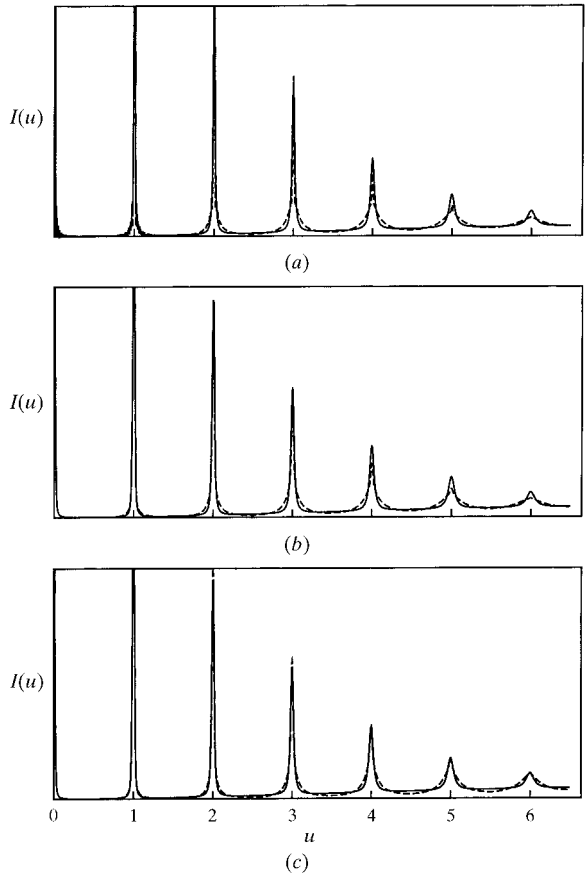

Figure 7
Diffraction patterns from generalized paracrystalline (full line) and perturbed lattice (dashed line) models for the 'worst case' ($N = 50$, $R = 2$, $\delta_{\rm pc} = 0.05$) for (*a*) $\delta_{\rm pl} = \delta_{\rm pc}$ without smearing, (*b*) $\delta_{\rm pl} = \delta_{\rm pc}$ with smearing, and (*c*) $\delta_{\rm pl} \neq \delta_{\rm pc}$ with smearing, as described in the text.

The terms inside each average in (30) are now each products of independent variables of the form $\exp(i2\pi ud)$ and the averages can therefore be evaluated, giving

$$I_{\rm pc}(u) = N + \exp(-4\pi^2u^2\sigma_{\rm nc}^2)\times\sum_{j=0}^{N-1}\left\{\sum_{k=0}^{j-1}\exp[i2\pi ua(j-k)]\exp[-2\pi^2u^2\sigma_{\rm pc}^2(j-k)] + \sum_{k=j+1}^{N-1}\exp[i2\pi ua(j-k)]\exp[-2\pi^2u^2\sigma_{\rm pc}^2(k-j)]\right\}. \quad (31)$$

The two summations over k can now be combined, giving

$$I_{\rm pc}(u) = N + 2\exp(-4\pi^2u^2\sigma_{\rm nc}^2)\sum_{j=0}^{N-1}\sum_{k=0}^{j-1}\exp[-2\pi^2u^2\sigma_{\rm pc}^2(j-k)]\times\cos[2\pi ua(j-k)], \quad (32)$$

and adding together terms of the same $(j-k)$ gives

$$I_{\rm pc}(u) = N + 2\exp(-4\pi^2u^2\sigma_{\rm nc}^2)\sum_{j=1}^{N-1}(N-j)\exp(-2\pi^2u^2\sigma_{\rm pc}^2j)\times\cos(2\pi uaj). \quad (33)$$

APPENDIX *B*
Perturbed lattice correlation coefficients

The relationship (11) for the correlation coefficient between kth nearest neighbors is a property of Markov chains that can be demonstrated as follows. Since we assume that only random variables at adjacent sites interact, the conditional density satisfies

$$P(d_j|d_{j-1}, d_{j-2}, \ldots, d_0) = P(d_j|d_{j-1}). \quad (34)$$

This is the Markov property, and the sequence $(d_0, d_1, \ldots)$ forms a Markov chain (Papoulis, 1991). Consider the random variables d_j and d_{j+k-1} $(k > 1)$. The d_j and d_{j+k-1} are jointly normal, and the correlation coefficient between them is denoted by q. The conditional density $P(d_{j+k-1}|d_j)$ is therefore

$$P(d_{j+k-1}|d_j) = P(d_{j+k-1}, d_j)/P(d_j) = \frac{1}{(2\pi)^{1/2}\sigma(1-q^2)^{1/2}}\exp\left[-\frac{(d_{j+k-1}-qd_j)^2}{2\sigma^2(1-q^2)}\right]. \quad (35)$$

Using the chain rule for conditional densities (Papoulis, 1991) and (34), the joint density $P(d_{j+k}, d_{j+k-1}, d_j)$ can then be written as

$$P(d_{j+k}, d_{j+k-1}, d_j) = P(d_{j+k}|d_{j+k-1})P(d_{j+k-1}|d_j)P(d_j), \quad (36)$$

which can be marginalized to give the joint density

$$P(d_{j+k}, d_j) = \int_{-\infty}^{\infty}P(d_{j+k}|d_{j+k-1})P(d_{j+k-1}|d_j)P(d_j)\,d\,d_{j+k-1}. \quad (37)$$

Since the perturbed lattice is stationary and $P(d_j)$ is normal, (35) can be used to evaluate (37) as

$$P(d_{j+k}, d_j) = \frac{1}{(2\pi)^{3/2}\sigma^3[(1-\rho^2)(1-q^2)]^{1/2}} \times \int_{-\infty}^{\infty} \exp\left[-\frac{(d_{j+k}-\rho d_{j+k-1})^2}{2\sigma^2(1-\rho^2)}\right] \times \exp\left[-\frac{(d_{j+k-1}-q d_j)^2}{2\sigma^2(1-q^2)}\right] \exp\left(-\frac{d_j^2}{2\sigma^2}\right) d\, d_{j+k-1}. \quad (38)$$

Expanding the arguments of the exponentials, completing the square of the terms involving d_{j+k-1} and changing the variable of integration allows (38) to be written in the form

$$P(d_{j+k}, d_j) = [2\pi^{3/2}\sigma^2(1-\rho^2q^2)^{1/2}]^{-1} \times \exp\left[-\frac{d_{j+k}^2 - 2\rho q d_{j+k} d_j + d_j^2}{2\sigma^2(1-\rho^2q^2)}\right] \times \int_{-\infty}^{\infty} \exp[-(x-b)^2]\,\mathrm{d}x, \quad (39)$$

where b is independent of x. Evaluating the integral gives

$$P(d_{j+k}, d_j) = \frac{1}{2\pi\sigma^2(1-\rho^2q^2)^{1/2}} \exp\left[-\frac{d_j^2 - 2\rho q d_j d_{j+k} + d_{j+k}^2}{2\sigma^2(1-\rho^2q^2)}\right], \quad (40)$$

so that the correlation coefficient is ρq. Equation (11) follows by mathematical induction and the fact that sites separated by $-k$ have the same statistics as those separated by k.

We are grateful to the US National Science Foundation for support (DBI-9722863).

References

Baltá-Calleja, F. J. & Hosemann, R. (1980). *J. Appl. Cryst.* **13**, 521–523.

Barakat, R. (1987). *Acta Cryst.* A**43**, 45–49.

Biswas, A. & Blackwell, J. (1988). *Macromolecules*, **21**, 3146–3151.

Brämer, V. R. (1975). *Acta Cryst.* A**31**, 551–560.

Egelman, E. H. & DeRosier, D. J. (1982). *Acta Cryst.* A**38**, 796–799.

Hall, I. H. & Somashekar, R. (1991). *J. Appl. Cryst.* **24**, 1051–1059.

Hammersley, J. M. (1967). *Proc. 5th Berkeley Symposium on Mathematical Statistics and Probability*, Vol. 3, pp. 89–118. Berkeley: University of California Press.

Hendricks, S. & Teller, E. (1942). *J. Chem. Phys.* **10**, 147–167.

Hosemann, R. (1950). *Z. Phys.* **128**, 465–492.

Hosemann, R. & Bagchi, S. (1962). *Direct Analysis of Diffraction by Matter.* Amsterdam: North-Holland.

Hosemann, R. & Hindeleh, A. (1995). *J. Macromol. Sci. Phys.* B**34**, 327–356.

Inouye, H. (1994). *Acta Cryst.* A**50**, 644–646.

Millane, R. P. & Stroud, W. J. (1991). *Int. J. Biol. Macromol.* **13**, 202–208.

Mu, X.-Q. (1998). *Acta Cryst.* A**54**, 606–616.

Mu, X.-Q., Makowski, L. & Fairchild, B. M. (1997). *Acta Cryst.* A**53**, 55–62.

Papoulis, A. (1991). *Probability Random Variables, and Stochastic Processes*, 3rd ed. New York: McGraw Hill.

Somashekar, R. & Somashekarappa, H. (1997). *J. Appl. Cryst.* **30**, 147–152.

Stroud, W. J. & Millane, R. P. (1995*a*). *Acta Cryst.* A**51**, 771–790.

Stroud, W. J. & Millane, R. P. (1995*b*). *Acta Cryst.* A**51**, 790–800.

Stroud, W. J. & Millane, R. P. (1996). *Proc. R. Soc. London Ser. A*, **452**, 151–173.

Welberry, T. R. (1985). *Rep. Prog. Phys.* **48**, 1543–1593.

Welberry, T. R. & Galbraith, R. F. (1973). *J. Appl. Cryst.* **6**, 87–96.

Welberry, T. R., Miller, G. H. & Carroll, C. E. (1980). *Acta Cryst.* A**36**, 921–929.